Available online www.worldscientificnews.com

World Scientific News

An International Scientific Journal

WSN 218 (2026) 10-26 EISSN 2392-2192

Role of Thin Layer of Dielectric Between Two Layers of Bilayer Graphene Superconductors

Hezekiah K. Cherop[1], Peter K. Tanui[2] and Kapil M. Khanna[3]

[1]Department of Physical, Biological and Health Sciences, Rongo University, P.O Box 103-40404, Rongo, Kenya

[2]Department of Education Science, Kabarak University, Private Bag-20157, Kabarak, Kenya

[3]Department of Physics, University of Eldoret, P.O Box 1125-30100, Eldoret, Kenya

Correspondence e-mail address: khannak700@gmail.com

https://doi.org/10.65770/UVWB1716

ABSTRACT

It has been found that a thin, high dielectric constant substrate can suppress superconductivity in twisted bilayer graphene (TBG). The high dielectric constant of substrate effectively screens and weakens the strong electronic interactions required for Cooper pair formation in TBG, thereby suggesting that the superconductivity in this system is driven by unconventional electronic interactions rather than the well-known phonon interactions. Using some of these ideas, the superconducting properties and parameters of bilayer graphene (BG), twisted bilayer graphene, and magic-angle-twisted-bilayer-graphene ($MATBG$), separated by a thin dielectric of thickness (d), are investigated under the assumption that the thickness of the upper and lower graphene layers are much greater than d, less than d or equal to d. Physical parameters such as heat capacity (C) and transition temperatures (T_c) were calculated for different values of energy gap (Δm) and geometric parameters ($r\ and\ d$). It was found that the heat capacity decreases monotonically with increasing temperature for both $r = d$ and $r > d$, indicating that thermal excitations are progressively suppressed as the energy gap increases, while in the case of $r < d$ a local enhancement that indicate a thermal crossover region was noted at T=250K. The calculated transition temperatures were noted to increase linearly with the energy gap for all the three models considered.

(Received 14 June 2026; Accepted 16 July 2026; Date of Publication 11 August 2026)

The derived model consistently predicted transition temperatures that lie between those of magic-angle twisted bilayer graphene (MATBG) and conventional bilayer graphene superconductors with a dielectric spacer. At the highest investigated energy gap ($\Delta m = 50.1\ meV$), the derived model predicts $T_c = 181.52K$ compared with $T_c = 119.03K$ for MATBG model and $T_c = 205.81K$ for the dielectric mediated BG model. These results indicate that the derived model captures the essential superconducting behavior of bilayer graphene while predicting a significant enhancement in superconducting performance relative to MATBG systems.

Keywords: Bilayer graphene, twisted bilayer graphene, magic-angle twisted bilayer graphene, dielectric constant, transition temperatures, energy gap.

1. INTRODUCTION

After the discovery of superconductivity in Mercury in 1911 [1], a large number of different types of superconductors have been fabricated and their properties have been studied from time to time both experimentally and theoretically [2-7]. The most successful theory of superconductivity was proposed by Bardeen-Cooper-Schrieffer, called BCS-theory [4] was based on the formation of electron pairs in which two-electrons come together to form a pair, called Cooper pair and the two electrons are bound to each other by the virtual exchange of a phonon. The BCS-theory could explain the superconducting properties of pure metals, metallic alloys, and doped semiconductors very successfully. Such superconductors are called conventional. All other types of superconductors, such as cuprates or high-T_c superconductors, heavy fermion superconductors, bilayer graphene superconductors, spin fluctuation superconductors etc., are called unconventional superconductors, and BCS theory is unable to explain their properties. In the large number of superconductors that have been fabricated and studied experimentally, it is found that each superconductor has a structure of its own, with different transition temperature (T_c), different variation of specific heat (C_v) and entropy (S), but what is common among all the superconductors is that the superconducting current is due to the formation of electron pairs, called the Cooper pairs, in the lowest superconducting state [5, 7].

Then with the discovery of cuprate superconductors [6] or high-T_c superconductors, it was found that a large number of semiconductors and insulators become superconductors at relatively high temperatures when compared to BCS type superconductors. It was found that the electron-electron pairing was not via the virtual exchange of phonons, but some sort of exotic pairing [5, 7]. Different types of unconventional superconductors have different transition temperatures (T_c), and specific heat(C_v) variations is also different for different superconductors. Some unconventional superconductors have low transition temperatures [8-11]. Another set of superconductors are called electron–hole superconductors whose properties have been studied recently [12]. Incidentally, there is still no single theory with unique electron pairing that can explain the properties of all types of superconductors.

Another material that has been studied extensively as a potential superconductor is graphene [13]. Bilayer graphene (BG), twisted bilayer graphene (TBG), and magic-angle-twisted-bilayer-graphene ($MATBG$) become superconductors when the superconductor is composed of two ultra-thin monolayer graphene super-lattice layers stacked above each other; the graphene layers are separated by an ultra-thin dielectric $(1\text{Å} = 10^{-8}cm)$that is sandwiched between the graphene layers. The whole arrangement is called Bernal stacking, and it is a quasi-two-dimensional system.

The electrons in both the layers may form unconventional electron-mediated pairing or exotic pairing [14-17]. Due to the proximity of the electrons in the Cooper pair, there will exist gravitational interaction with a cut off equal to the coherence length (ξ) of the Cooper pairs. Alternatively, there could exist electroweak gravitational interaction (with constant $G_g = 2.909 \times 10^{22} Nm^2/kg^2$), and or electromagnetic interaction (with constant $G_e = 2.374 \times 10^{37} m^3/kgSec^2$) [18]. It is also possible that there may exist novel particles of extremely heavy mass of the order of $10^{37} GeV$ that keep the two electrons together in a Cooper pair. Another possibility is the existence of a weak fermion of some rest energy that binds the charges in the Cooper pair, and even the charge (e_n) in the Cooper pair may be such that $e_n = 2.946e$ where e is the electron charge. The related parameter of interest is the energy of the Cooper pair ($10^{-3} eV$ as pairing interaction), and this is attractive to keep the Cooper pair bound.

An important experimental observation that was done long ago [19] show that in all superconductors, the magnetic flux quantum, $\phi_o = \frac{h}{2e}$, is the same since it is composed of two universal constants h and e, and this magnetic flux quantum (ϕ_o) is a consequence of the motion of Cooper pairs that carry the electric charge $2e$. Thus, it is reasonable to surmise that the interaction between the charges (electrons) in the Cooper pairs should be the same and composed of some universal constants for all types of superconductors since nature will not choose different forms of interaction between the electrons in the Cooper pairs. Moreover, electrons have no eyes to decide in which superconductor they are moving, they have only one choice and that is that they form Cooper pairs in the superconducting state. Having said that, we now mention some of the important parameters that describe the complexion of superconductors [5, 7, 11];

- Transition temperatures (T_c) is the temperature at which a material changes from normal to superconducting state.
- H_{C1} and H_{C2} are the magnetic field limits that determine the stability or destruction of the superconducting state.
- Coherence length (ξ) refer to length up to which electrons in Cooper pairs remain correlated.
- Energy gap (Δ) refers to the energy at the Fermi surface.

But an important parameter that has been added in the case of bilayer graphene superconductor is the very thin dielectric sheet of thickness $d \cong 10^{-8} cm$ between the two layers of the graphene superconductors. The exact role of this thin dielectric sheet in determining the properties of the bilayer graphene superconductors is not clearly known or mentioned anywhere in the literature available so far. We have tried to study the effect of varying the thickness of the dielectric on the properties, such as specific heat (C_v) and transition temperatures (T_c). The theoretical values of C_v and T_c are compared with the experimental values known so far [20-24]. Additionally, some details of the effect of variation of dielectric thickness and its magnitude are mentioned below.

2. ROLE OF DIELECTRIC BETWEEN TWO GRAPHENE LAYERS.

It is well known that dielectric constant (k) increases with increasing thickness for up to around $500nm$ thickness, and then it almost becomes independent of thickness. The theory shows that the decrease of dielectric permittivity with decreasing thickness is directly caused by the restriction in space of the available eigenmodes for the field-induced alignment of ions and charge groups [25]. The three inner barrier dielectrics that have been used in bilayer graphene superconductors are $h-BN(k=4)$, $Al_2O_3(k=12.53)$ and $HfO_2(k=22)$. The charge mobilities of these dielectrics depend on the interlayer distance d [26].

In this experiment the impurity concentration (n_i) was chosen as $n_i = 5 \times 10^{11} cm^{-2}$, and the carrier concentration (n_c) was chosen as $n_c = 10^{12} cm^{-2}$. The charged impurity scattering rate was different for each dielectric. Here the value of d for each dielectric was $d \cong 10^2 nm = 10^{-5} cm$. Thus in this system two graphene separated by a dielectric barrier layer, and that the carrier mobility strongly depends on the dielectric constant of the barrier layer when the interlayer distance becomes larger than the inverse of the Fermi wave vector (k_F) [26]. Several electronic transport measurements on atomically-thin materials, and or graphene, have shown mobility enhancement effect on the carrier mobility through change in dielectric environment [27]. Thus changes in dielectric constant (k) lead to changes in carrier mobility.

Dependence of mobility on the interlayer distance (d) or thickness of dielectric has also been studied. For smaller interlayer distance, $d \cong 0.1\, nm = 10^{-8} cm = 1$Å, the mobilities are independent of the distance (d). With increasing interlayer distance when $d \cong 10nm = 10^{-6} cm$, the effects on the mobility become prominent, and the carrier mobillities strongly depend on large d values because the interlayer Coulomb interaction becomes negligible due to large d. Thus the carrier mobilities can be improved by inserting higher value dielectrics (with larger thickness) as the middle layer between two graphene layers (dielectric constant k increases as d increases up to about $500nm$). Thus a proper combination of dielectric thickness and dielectric constant can be chosen to improve upon the mobility for graphene-double layer-structure (GDLS), especially for a thinner GDLS [28].

Now it is important to point out that the interlayer relative dielectric constant $(k_r \; or \; \epsilon_r)$ of the two dimensional $(2D)$materials, and or graphitic materials in particular, is one of the most important physical properties for electric applications; and the superconducting properties of such materials [28]. In general, the graphitic contacts are in the nanoscale $\left(10^{-9}\, m = 10^{-7} cm = 10\text{Å}\right)$. It is found that the intrinsic dielectric constant (ϵ_r) of the bilayer graphene interface is $\epsilon_r = 6 \pm 2$. This agrees with the recent theoretical predictions for multilayer graphene structures. The dielectric constant is one of the essential characteristics that characterize the electrostatic properties of materials. Properties such as capacitance, charge screening, energy storage and electron-electron interaction are essentially described by the ability of a material and its surroundings to re-arrange charge. In graphene, Coulomb interactions play a significant role especially near the charge neutrality point (CNP) where the screening length diverges [29]. Studies have shown the crucial role of dielectric screening in graphene to control both Fermi velocity (V_F) and electron-electron interactions [30]. Studies have also been done on the unique phenomena such as tunable band gap in bilayer and trilayer graphene, superconducting-insulating transitions, Coulomb drag and gate controlled surface plasmons pointing out to a strong interplay between graphene properties and external electric fields. Thus the values of the dielectric constants of graphene and that of the dielectric between the two layers of graphene in a bilayer system has led to great interest in this field.

Different experiments have found large variation in the range of values of relative permittivity (ϵ_r) such that $\epsilon_r$varies from 2 to 15. The ultra-thin nature of graphene and the presence of substrates has played a great role in the experimental attempts to measure its intrinsic dielectric constant [31]. It is also found that different angular configurations between the top and the bottom flakes will induce different electronic coupling that can essentially induce variations in the measured dielectric properties, and these can lead to variations in the transition temperature (T_c) and specific heat (C_v) to the superconducting state. Studies with precise control over the angular mismatch and interlayer coupling can reveal their impact on the dielectric properties in the 2D graphene system.

Our aim in this manuscript is to study the role of thin layer of dielectric between the two layers of the bilayer graphene superconductor, especially to calculate how the specific heat (C_v) and transition temperature (T_c) vary with changes in the magnitude of the thickness of dielectric (d) that is sandwiched between the layers.

3. THEORETICAL DERIVATIONS

From our knowledge of the detailed analysis about the properties of unconventional superconductors, and now the superconductivity in bilayer graphene graphene (BG), twisted bilayer graphene (TBG), and magic-angle-twisted-bilayer-graphene $(MATBG)$, it is clear that we have landed ourselves in a marshland of superconductivity; the more we go deep into it, the more we are unable to successfully come out of it. There are around 100 unsolved problems in Physics, the phenomena of unconventional could as well be the hundred-one-th unsolved problem in Physics. We have still not been able to develop a theory that can explain uniquely the properties of all types of unconventional superconductors. Even then, it is said that at its best, Physics eliminates complexity by revealing the underlying simplicity.

Now it is generally believed that new Physics emerges when two energy scale can be compared with each other. The two energy scales in superconductivity are (i) Energy gap (Δ) in the single-particle energy excitation spectrum and (ii) Binding energy of the Cooper pair. When these two quantities are equal, or roughly equal, one can observe phase transition to the superconducting state.

In this manuscript, we will look for the energies involved in a bilayer-graphene(BG) superconductor in which the two graphene layers are separated by a dielectric of very small thickness $(10^{-8}cm)$. The study concentrates on how the variations in the thickness of the dielectric affects the specific heat (C_v) and transition temperature (T_c). The doping of graphene layers may be such that the electrons may flow in one layer, and holes may flow in the second layer; or in both the graphene layers, electrons may flow. Cooper pairs will be formed between the charges of each layer, and the separation distance between the charges in the Cooper pair may be the thickness of the dielectric or a little more.

We will now assume that there are two main energies involved in this phenomena of superconductivity of a bilayer-graphene system with a dielectric in between the layers. One is the modified Coulomb energy between the charges in the Cooper pairs and the second is the Bogoliubov quasi-particle energy. The Bogoliubov quasi-particles are elementary excitations above the ground state.

The Coulomb energy between two charges of magnitude $|e|$, and separation r is given by;

$$E_c = \frac{e^2}{4\pi\epsilon_0 r} \tag{1}$$

Where ϵ_0 is permittivity of free space. Due to proximity of charges in Cooper pairs, the modified Coulomb energy E_m is written as [24,32]

$$E_m = E_c e^{-\alpha r} \tag{2}$$

Where α is some constant that is determined by the condition that will determine the range of the Coulomb interaction and its relation to the coherence length(ξ) of the charges in the Cooper pair. In the bilayer graphene superconductor, the range of the Coulomb interaction is assumed to be the size of the dielectric thickness (d) between the graphene layers. This is the minimum distance between the charges in the Cooper pair [33].

The coherence length(ξ) could be quite large, in the range $96nm$ $(960Å)$to $113nm$ $(1130Å)$[34]. Thus the range of the Coulomb interactions say r_c, can vary between 1Å to 1130Å, which is a large range. Now considering that the variation of E_m at $r = r_c$ will be zero, we can write;

$$\left(\frac{\partial E_m}{\partial r}\right)_{r=r_c} = 0 \tag{3}$$

This lead to,

$$\alpha = -\frac{r}{{r_c}^2} = -\frac{r}{d^2} \tag{4}$$

And hence,

$$E_m = E_c e^{\frac{r^2}{d^2}} \tag{5}$$

For $r = d$, we get,

$$E_m = E_c e = 2.718E_c \tag{6}$$

As per this calculations, the Coulomb interaction between the charges in the Cooper pair is larger by a factor of Napierian logarithm $e = 2.718$. The value of r is calculated using the following well known relation;

$$r = \frac{\hbar V_F}{\pi \Delta_0} \tag{7}$$

where, $\Delta_0 = 1.764kT_c = Energy\ gap.$

The second part of the energy is the Bogoliubov quasi-particle energy which is obtained by writing the corresponding part of the Hamiltonian and diagonalizing it using the Bogoliubov canonical transformation [24, 35]. The expression for the quasi-particle energy multiplied by the quantum-mechanical thermal-activation factor is E_k, i.e,

$$E_k = \frac{2\pi N_0 k^2}{T^3} e^{-\frac{\Delta m}{kT}} \tag{8}$$

The sum of Equation (5) and Equation (8) will give the total energy E of the bilayer graphene superconductor with a dielectric layer between the graphene layers, i.e,

$$E = \left(E_c e^{\frac{r^2}{d^2}} + \frac{2\pi N_0 k^2}{T^3}\right) e^{-\frac{\Delta m}{kT}} \tag{9}$$

Here $N_0 = layer\ number\ charge\ density = 2 \times 10^{28} cm^{-2}$

The specific heat, C, is given by

$$C = \frac{\partial E}{\partial T} = \left[E_c e^{\frac{r^2}{d^2}} \left(\frac{\Delta m}{kT^2}\right) - \frac{6\pi N_0 k^2}{T^4} + \frac{2\pi N_0 k^2 \Delta m}{kT^5}\right] e^{-\frac{\Delta m}{kT}} \tag{10}$$

The transition temperature, T_c , is determined as ;

$$\left(\frac{\partial C}{\partial T}\right)_{T=T_c} = 0 \tag{11}$$

The entropy can be determined as;

$$S = \int C dT \tag{12}$$

Equation (10) gives the expression for the specific heat C as a function of a number of parameters that determine the structure of the superconductor and the characteristics of the superconductor. For a given experiment, N_0 and d will be fixed or constant. Here r is the distance between the charges in the Cooper pair, and is calculated using Equation (7).

The value of Δm is fixed from the relation $\Delta_0 = 1.764kT_c$. In $MATBG$, superconducting energy gaps are small in the range of $0.1\ meV$ to $0.5\ meV$, and the ratio $\frac{2\Delta_0}{kT_c} = 6.1$ compared to $\frac{2\Delta_0}{kT_c} = 3.528\ (2 \times 1.764)$ which means strong coupling. To make things simple, we use the first term in Equation (10) and Equation (11) to calculate C and T_c respectively.

For transition temperatures, our derivation gives;

$$T_c = \frac{\Delta m}{2k} \tag{12}$$

For $MATBG$ superconductor, the general expression for transition temperatures is written as;

$$T_c = \frac{2\Delta m}{6.1k} \tag{13}$$

Additionally, the general expression for bilayer graphene superconductor with dielectric between the layers is written as;

$$T_c = \frac{\Delta m}{1.764k} \tag{14}$$

4. RESULTS AND DISCUSSIONS

The Heat capacity (C) was calculated for different values of d and the energy gap (Δm). The Δm values were varied from $0.1\ meV$ to $50\ meV$ in increments of $5\ meV$. For $N_0 \cong 10^{18} particle\ cm^{-2}$, $\Delta m \cong 0.71 \times 10^{-7} eV$. Here, Δm represents the energy gap at $T = 0$ or at the Fermi energy ϵ_F. The calculated heat capacities corresponding to different values of the ratio $\frac{r^2}{d^2}$ are presented in Table 1, Table 2 and Table 3. The results in Table 1 presents the calculated heat capacities for different values of temperature, energy gap (Δm), and geometric ratios $r = d$. At $T = 0K$, the heat capacity is undefined, which is consistent with thermodynamic expectations since no thermal excitations are available at absolute zero. As the temperature increases from 50 K to 500 K, the heat capacity decreases continuously.

Table 1. Heat Capacities for $r = d$.

T (K)	**Δm(meV)**	**Δm(erg)**	**r (cm)**	**d (cm)**	***Heat Capacity*** $(\frac{erg}{K})$ $\boldsymbol{r = d}$
0	0.1	1E-16	1E-10	1E-10	-
50	5.1	5.1E-15	5E-10	5E-10	8.853E-14
100	10.1	1.01E-14	1E-09	1E-09	2.207E-14
150	15.1	1.51E-14	1.5E-09	1.5E-09	9.802E-15
200	20.1	2.01E-14	2E-09	2E-09	5.511E-15
250	25.1	2.51E-14	2.5E-09	2.5E-09	3.526E-15
300	30.1	3.01E-14	3E-09	3E-09	2.448E-15
350	35.1	3.51E-14	3.5E-09	3.5E-09	1.799E-15
400	40.1	4.01E-14	4E-09	4E-09	1.377E-15
450	45.1	4.51E-14	4.5E-09	4.5E-09	1.088E-15
500	50.1	5.01E-14	5E-09	5E-09	8.811E-16

The graphical illustration for the results in Table 1 $(r = d)$ is shown in Figure 1. This graph exhibits a smooth, monotonically decreasing trend in heat capacity as temperature increases from 50 K to 500 K. The heat capacity decreases rapidly at lower temperatures and then gradually approaches very small values in the order of $10^{-16} erg/K$ at higher temperatures. This behavior indicates that thermal excitations become progressively suppressed as the energy gap in Δm increases. The steep decline between approximately 50 K and 150 K may indicate the onset of a thermal crossover region where quasiparticle excitations become increasingly restricted. Beyond about 250 K, the curve flattens considerably, suggesting that the heat capacity has entered a nearly saturated low-value regime. The absence of a sharp peak suggests that no strong second-order phase transition is observed within the investigated temperature range. Instead, the system exhibits a gradual reduction in thermal response, characteristic of a gapped quasiparticle spectrum where fewer excitations contribute to the specific heat as temperature increases.

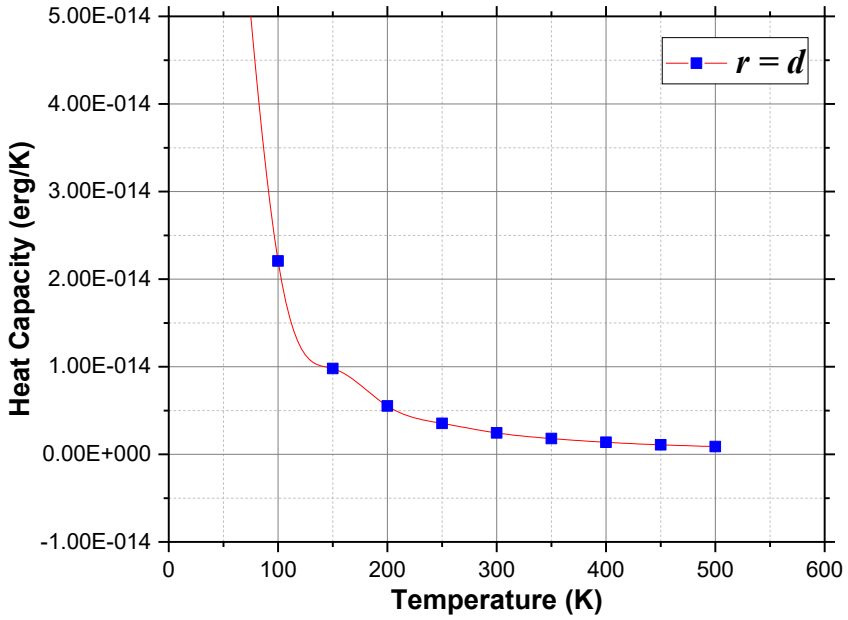

Figure 1. Graph of Heat Capacities against Temperature for $r = d$.

In Table 2, we consider the case where $r > d$. It is noted that the values of heat capacities obtained when $r > d$ are larger than those for $r = d$. This behavior arises from the exponential geometric factor $e^{\frac{r^2}{d^2}}$, which becomes significantly greater than unity when $r > d$. Consequently, the spatial separation parameter r enhances the thermal energy contribution, leading to larger heat-capacity values. The enhancement indicates that the system becomes more sensitive to thermal fluctuations when the characteristic radius exceeds the interaction length scale.

Table 2. Heat Capacities for $r > d$.

T (K)	**Δm(*meV*)**	**Δm(erg)**	**r (cm)**	**d (cm)**	***Heat Capacity*** $(\frac{erg}{K})$ $r > d$
0	0.1	1E-16	1E-10	0.5E-10	-
50	5.1	5.1E-15	5E-10	3E-10	5.238E-13
100	10.1	1.01E-14	1E-09	5E-10	4.434E-13
150	15.1	1.51E-14	1.5E-09	7E-10	3.558E-13
200	20.1	2.01E-14	2E-09	9E-10	2.829E-13

250	25.1	2.51E-14	2.5E-09	1.1E-09	2.271E-13
300	30.1	3.01E-14	3E-09	1.3E-09	1.851E-13
350	35.1	3.51E-14	3.5E-09	1.5E-09	1.532E-13
400	40.1	4.01E-14	4E-09	1.7E-09	1.285E-13
450	45.1	4.51E-14	4.5E-09	1.9E-09	1.092E-13
500	50.1	5.01E-14	5E-09	2.1E-09	9.391E-14

Similarly, the graphical illustration for the results in Table 2 $(r > d)$ is shown in Figure 2. In Figure 2 the curve is smoother and more extended because the geometric factor amplifies the thermal contribution. The higher values imply that spatial effects represented by $\frac{r^2}{d^2}$ increase the sensitivity of the system to thermal fluctuations. However, the same suppression mechanism associated with the increasing energy gap eventually dominates, causing the heat capacity to decrease steadily. Hence, the graph does not exhibit a pronounced lambda-shaped peak or divergence that would typically signify a well-defined phase transition.

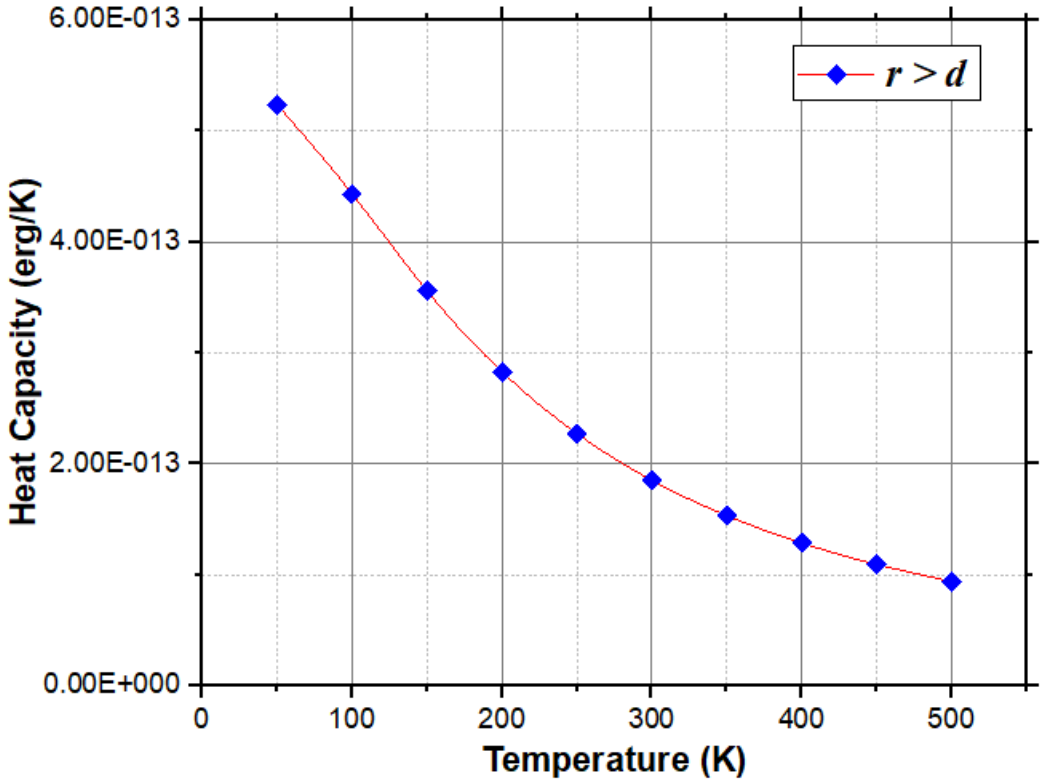

Figure 2. Graph of Heat Capacities against Temperature for $r > d$.

In Table 3, we consider the case when $r < d$. Similar to the cases $r = d$ and $r > d$, the heat capacity and energy gap decreases steadily with increasing temperature, falling from $5.425 \times 10^{-14} erg/K$ at 50 K to $8.171 \times 10^{-16} erg/K$ at 500K. This trend indicates that the thermal response of the system becomes progressively weaker as the temperature and energy gap increase, reducing the number of thermally accessible quasiparticle states.

Table 3. Heat Capacities for $r < d$.

T (K)	**Δm(meV)**	**Δm(erg)**	**r (cm)**	**d (cm)**	***Heat Capacity*** $(\frac{erg}{K})$ $r < d$
0	0.1	1E-16	1E-10	1.5E-10	-
50	5.1	5.1E-15	5E-10	7E-10	5.425E-14
100	10.1	1.01E-14	1E-09	1.2E-09	1.626E-14
150	15.1	1.51E-14	1.5E-09	1.7E-09	7.855E-15
200	20.1	2.01E-14	2E-09	2.2E-09	4.633E-15
250	25.1	2.51E-14	2.5E-09	2.7E-09	1.128E-14
300	30.1	3.01E-14	3E-09	3.2E-09	2.169E-15
350	35.1	3.51E-14	3.5E-09	3.7E-09	1.619E-15
400	40.1	4.01E-14	4E-09	4.2E-09	1.255E-15
450	45.1	4.51E-14	4.5E-09	4.7E-09	1.001E-15
500	50.1	5.01E-14	5E-09	5.2E-09	8.171E-16

Compared with the $r = d$ case in Table 1, the heat-capacity values in Table 3 are generally larger at lower temperatures. This increase arises from the geometric factor $e^{\frac{r^2}{d^2}}$, which still contributes positively to the heat capacity even though $r < d$. Since $\frac{r^2}{d^2} < 1$, the exponential enhancement is weaker than in the $r > d$ case, but it remains sufficient to increase the thermal energy contribution relative to the $r = d$ configuration. Consequently, the heat capacities for $r < d$ lie between those obtained for $r = d$ and $r > d$, reflecting the intermediate influence of the geometric factor.

A slight deviation from the general decreasing trend is observed at T=250 K as shown in Figure 3, where the heat capacity increases to $1.128 \times 10^{-14} erg/K$ from $4.633 \times 10^{-15} erg/K$ at 200K.

This anomaly may be associated with effects arising from the competing influences of temperature, energy gap, and geometric parameters leading to thermal crossover region where quasiparticle excitations become increasingly restricted. Although this local enhancement may indicate a thermal crossover region associated with the competition between thermal energy, the superconducting energy gap, and geometric confinement effects, it does not constitute clear evidence of a phase transition. A genuine phase transition is typically characterized by a pronounced discontinuity or peak in the heat-capacity curve. The observed anomaly is therefore more likely related to a temporary redistribution of quasiparticle excitations within the system. Beyond T=250 K, the heat capacity resumes its decreasing behavior, indicating that thermal excitations become increasingly suppressed as the superconducting gap widens.

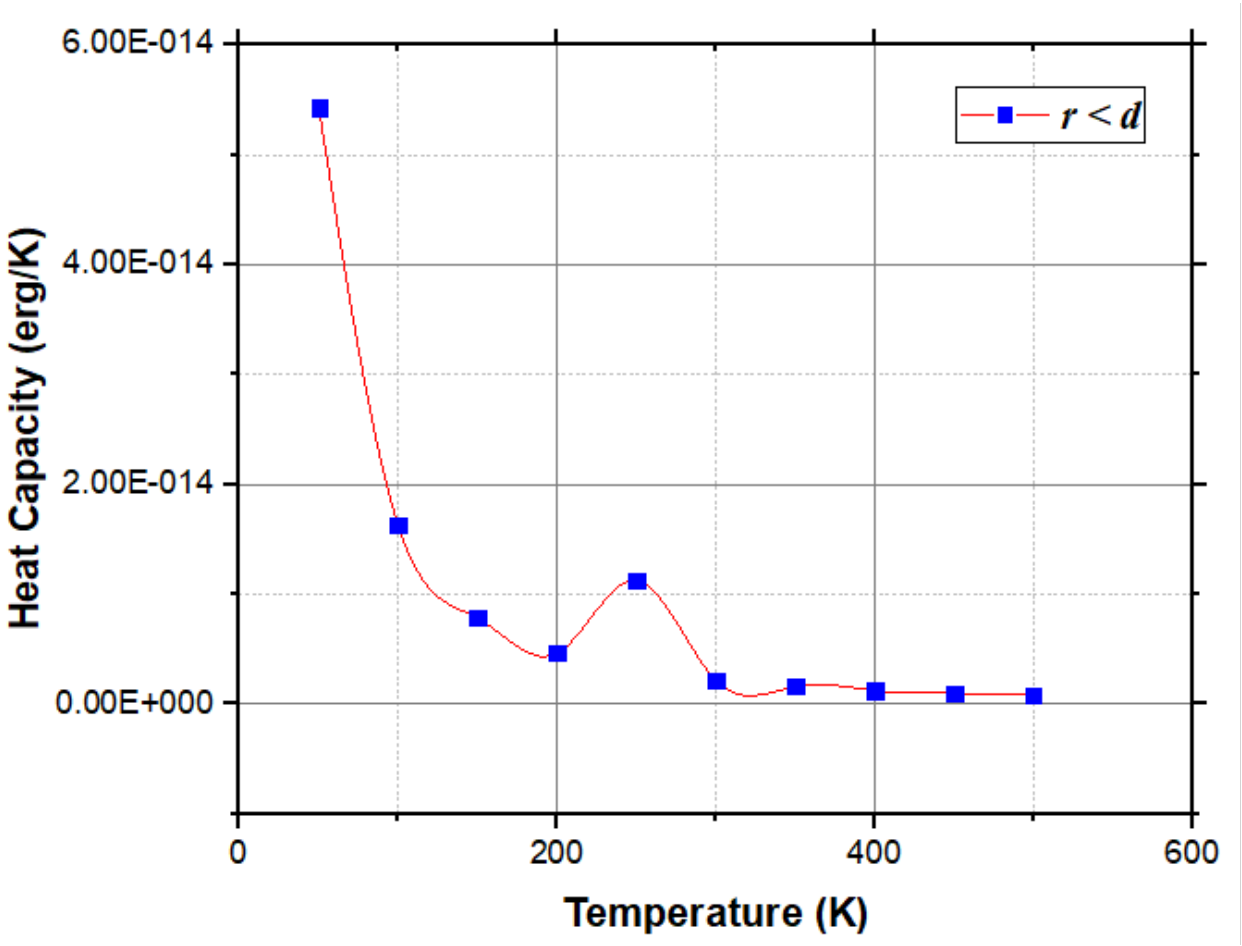

Figure 3. Graph of Heat Capacities against Temperature for $r < d$.

The decrease in heat capacity with increasing temperature in Table 1, Table 2 and Table 3, despite the increase in Δm, suggests that the exponential suppression factor $e^{-\frac{\Delta m}{kT}}$ dominates the thermal response. As the energy gap increases, fewer quasiparticle excitations are thermally activated, reducing the amount of energy absorbed per unit temperature change.

The calculations for transition temperatures (T_c) were obtained using Equations (12), (13), and (14), respectively and the results are shown in Table 4. These results represent the transition temperatures for three different models of bilayer graphene superconductors: the derived model proposed in this work, the magic-angle twisted bilayer graphene (MATBG) superconductor model, and the bilayer graphene (BG) superconductor model with a dielectric layer between the graphene sheets.

Table 4. Transition Temperatures for derived model of BG superconductors, MATBG and BG Superconductors.

Transition Temperatures (K)		
Derived model	**MATBG Superconductor.**	**BG Superconductor**
0.36	0.24	0.41
18.48	12.12	20.95
36.59	24.00	41.49
54.71	35.88	62.03
72.83	47.75	82.57
90.94	59.63	103.11
109.06	71.51	123.65
127.17	83.39	144.19
145.29	95.27	164.73
163.41	107.15	185.27
181.52	119.03	205.81

The results in Table 4 suggest that the derived model reproduces the general behavior expected for graphene-based superconductors while remaining reasonably close to the conventional bilayer graphene prediction. For example, at the highest investigated energy gap ($\Delta m = 50.1\, meV$), the derived model predicts $T_c = 181.52K$ compared with $T_c = 205.81K$ for the BG model and $T_c = 119.03K$ for the MATBG model. This indicates that the derived model captures a substantial enhancement of superconductivity relative to MATBG while remaining somewhat more conservative than the dielectric-mediated BG model.

Another important observation from our calculations is that the differences between the three models become increasingly pronounced as Δm increases. At low energy gaps, the discrepancies are only fractions of a kelvin, but at larger energy gaps the differences exceed tens of kelvin. This demonstrates that the choice of theoretical model becomes increasingly significant when predicting high-temperature superconductivity.

5. CONCLUSIONS

The heat capacity and transition temperatures of bilayer graphene superconductors were investigated for different energy gaps (Δm) and geometric parameters $(r\ and\ d)$. The results show that the heat capacity decreases monotonically with increasing temperature for both $r = d$ and $r > d$, indicating that thermal excitations are progressively suppressed as the energy gap increases. The observed gradual reduction in heat capacity points to a thermal crossover regime associated with the suppression of quasiparticle excitations in a gapped superconducting state. Additionally, the larger heat-capacity values obtained for $r < d$ demonstrate that the geometric factor $e^{\frac{r^2}{d^2}}$ significantly enhances the thermal response of the system, highlighting the importance of spatial separation effects in determining the thermodynamic properties of bilayer graphene superconductors. In the case of $r < d$, a slight deviation from the general decreasing trend is observed at T=250 K. This anomaly may be associated with effects arising from the competing influences of temperature, energy gap, and geometric parameters where quasiparticle excitations become increasingly restricted. Although this local enhancement may indicate a thermal crossover region associated with the competition between thermal energy, the superconducting energy gap, and geometric confinement effects, it does not constitute clear evidence of a phase transition. Generally, in superconducting systems, a phase transition is normally identified by a pronounced anomaly in the heat capacity at the critical temperature T_c. For a second-order superconducting transition, the heat capacity typically exhibits a discontinuity or peak near T_c, rather than a small isolated fluctuation.

The calculated transition temperatures in this study were found to increase linearly with the energy gap for all the three models considered. The derived model consistently predicted transition temperatures that lie between those of magic-angle twisted bilayer graphene (MATBG) and conventional bilayer graphene superconductors with a dielectric spacer. At the highest investigated energy gap $(\Delta m = 50.1\ meV)$, the derived model predicts $T_c = 181.52K$ compared with $T_c = 119.03K$ for MATBG model and $T_c = 205.81K$ for the dielectric mediated BG model. These results indicate that the derived model captures the essential superconducting behavior of bilayer graphene while predicting a significant enhancement in superconducting performance relative to MATBG systems.

Overall, the study demonstrates that both the superconducting energy gap and the geometric factor $\frac{r^2}{d^2}$ play crucial roles in determining the thermal and superconducting properties of bilayer graphene. The derived model provides physically consistent predictions and suggests the possibility of achieving relatively high transition temperatures through appropriate control of pairing strength and interlayer interactions, making it a useful framework for investigating superconductivity in graphene-based materials. Superconducting transition temperatures for bilayer graphene show considerable variation depending upon the structure of the bilayers, the dielectric between the layers, and the angle of twist between the bilayers $(MATBG)$. Transition temperatures can be in the range $30mK$ to $1.5K$, $3K$, and by increasing structural disorder, it can be shifted to room temperatures $(300K)\ or\ 27^0C$ [36]. Therefore, thinner dielectrics increase Coulomb screening (since Coulomb repulsion increases for thin dielectric or small d), and reduce attractive potential thereby suppressing the pairing interaction and hence lowering T_c, while thicker dielectrics can optimize T_c by minimizing this destructive screening (since thicker dielectric-larger d reduces Coulomb Potential and increases binding of electron pairs, and hence increase in T_c).

References

[1] Onnes, H. K., Leiden Comm. *Nos.* (1911) *122b, 124c, 133a, 133c*.

[2] Meissner, W., & Ochsenfeld, R. Ein neuer effekt bei eintritt der supraleitfähigkeit. *Naturwissenschaften*,*21*(44), (1933)787-788.

[3] Cooper, L. N., Bound electron pairs in a degenerate Fermi gas. *Physical Review*, *104*(4) (1956) 1189.

[4] Bardeen, J., Cooper, L. N., & Schrieffer, J. R., Theory of superconductivity. *Physical review*, *108*(5) (1957) 1175.

[5] Mourachkine, A., *Room-temperature superconductivity*. Cambridge Int Science Publishing (2004).

[6] Bednorz, J. G., & Müller, K. A., Possible high T c superconductivity in the Ba− La− Cu− O system. *Zeitschrift für physik B condensed matter*, *64*(2) (1986) 189-193.

[7] Khanna, K., Inaugural lecture on Superconductivity, Moi University, Kenya (2008).

[8] Steiner, C. M., Heavy Fermion Superconductivity‖. *Phys. Rev*, *569* (2011) 027003.

[9] White, B. D., Thompson, J. D., & Maple, M. B., Unconventional superconductivity in heavy-fermion compounds. *Physica C: superconductivity and its applications*, *514* (2015) 246-278.

[10] Bauer, E., Hilscher, G., Michor, H., Paul, C., Scheidt, E. W., Gribanov, A., ... & Rogl, P., Heavy fermion superconductivity and magnetic order in noncentrosymmetric, *Physical review letters*, *92*(2) (2004) 027003.

[11] Tinkham, M., *Introduction to superconductivity*. Courier Corporation (2004).

[12] Tanui, P. K., Namwetako, J. S., Ingosy, A., & Khanna, K. M, Superconductivity and Electron-Hole Superconductivity. *International Journal of Recent Research Aspects*, *7*(3) (2020) 14-19.

[13] Bhatia, I. S., & Randhawa, D. K. K., Something more than graphene–futuristic two-dimensional nanomaterials. *Current Science*, *118* (11) (2020) 1656-1671.

[14] Isabelle D., Magic-angle graphene behaves like high-temperature superconductor, 2D materials. Physics World, (2018).

[15] You, Y. Z., & Vishwanath, A., Superconductivity from valley fluctuations and approximate SO (4) symmetry in a weak coupling theory of twisted bilayer graphene. *npj Quantum Materials*, *4*(1) (2019)16.

[16] Iwasaki, T., Morita, Y., Nakaharai, S., Wakayama, Y., Watanabe, E., Tsuya, D., ... & Moriyama, S., Fabrication of folded bilayer-bilayer graphene/hexagonal boron nitride superlattices. *Applied Physics Express*, *13*(3) (2019) 035003.

[17] Islam, S. F., Zyuzin, A. Y., & Zyuzin, A. A., Unconventional superconductivity with preformed pairs in twisted bilayer graphene. *Physical Review B*, *107*(6) (2023) L060503.

[18] Onofrio, R., On weak interactions as short-distance manifestations of gravity. *Modern Physics Letters A*, *28*(07) (2013)1350022.

[19] Doll, R., & Näbauer, M., Experimental proof of magnetic flux quantization in a superconducting ring. *Physical Review Letters*, *7*(2) (1961) 51.

[20] Hazra, T., Verma, N., & Randeria, M., Bounds on the superconducting transition temperature: Applications to twisted bilayer graphene and cold atoms. *Physical Review X*, *9*(3) (2019) 031049.

[21] Bistritzer, R., & MacDonald, A. H., Transport between twisted graphene layers. *Physical Review B—Condensed Matter and Materials Physics*, *81*(24) (2010) 245412.

[22] Dinh, T. H., Characterization of Magic-angle Twisted Bilayer Graphene using Microwave Techniques, (2021).

[23] Kiboi D.C, Tanui P, Limo C.S and Khanna K.M., Electron- hole superconductivity in Bilayer Graphene superconductors. SITA, 2 (25) (2023).

[24] Kiboi, D. C., Samuel, L. C., & Khanna, K. M., Bogoliubov de Gennes (BdG) Hamiltonian for electron-hole superconductors. *World Scientific News*, (2022) 43-54.

[25] Zaccone, A., Explaining the thickness-dependent dielectric permittivity of thin films. *Physical Review B*, *109*(11), (2024) 115435.

[26] Hosono, K., & Wakabayashi, K., Dielectric environment effect on carrier mobility of graphene double-layer structure. *Applied Physics Letters*, *103*(3) (2013).

[27] Linh, D. K., & Khanh, N. Q., Charged impurity scattering in bilayer-graphene double layers. *International Journal of Modern Physics B*, *34*(27), (2020) 2050254.

[28] Bessler, R., Duerig, U., & Koren, E., The dielectric constant of a bilayer graphene interface. *Nanoscale Advances*, *1*(5), (2019) 1702-1706.

[29] Elias, D. C., Gorbachev, R. V., Mayorov, A. S., Morozov, S. V., Zhukov, A. A., Blake, P., ... & Geim, A. K., Dirac cones reshaped by interaction effects in suspended graphene. *Nature Physics*, *7*(9), (2011) 701-704.

[30] Hwang, C., Siegel, D. A., Mo, S. K., Regan, W., Ismach, A., Zhang, Y., ... & Lanzara, A., Fermi velocity engineering in graphene by substrate modification. *Scientific reports*, *2*(1) (2012) 590.

[31] Siegel, D. A., Park, C. H., Hwang, C., Deslippe, J., Fedorov, A. V., Louie, S. G., & Lanzara, A., Many-body interactions in quasi-freestanding graphene. *Proceedings of the National Academy of Sciences*, *108*(28), (2011) 11365-11369.

[32] Fil, D. V., & Kravchenko, L. Y., Superconductivity of electron–hole pairs in a bilayer graphene system in a quantizing magnetic field. *Low Temperature Physics*, *35*(8), (2009) 712-723.

[33] Cea, T., & Guinea, F., Coulomb interaction, phonons, and superconductivity in twisted bilayer graphene. *Proceedings of the National Academy of Sciences*, *118*(32), (2021) 2107874118.

[34] Hwang, J., Superconducting coherence length of hole-doped cuprates obtained from electron–boson spectral density function. *Scientific Reports*, *11*(1), (2021) 11668.

[35] Sarkar, S., Emergence of a new symmetry class for Bogoliubov-de Gennes (BdG) Hamiltonians: Expanding ten-fold symmetry classes. (2018). *arXiv preprint:1810.07618*.

[36] Ku, R, Yan L., High superconducting transition temperature in bilayer blue phosphorus by metal intercalation. *Physic Review B* 111, (2025) 234429.